Asociación Argentina
de Mecánica Computacional

Mecánica Computacional Vol XXXIII, págs. 453-472 (artículo completo)
Graciela Bertolino, Mariano Cantero, Mario Storti y Federico Teruel (Eds.)
San Carlos de Bariloche, 23-26 Setiembre 2014

WATER/OIL SEPARATION MODELING BY POPULATION BALANCE EQUATIONS - SOLUTION OF THE PROBABILITY DENSITY FUNCTION

Santiago Márquez Damián[a] **and Gustavo C. Buscaglia**[b]

[a]*Centro de Investigaciones en Mecánica Computacional (CIMEC), UNL/CONICET, Colectora Ruta Nac. 168 / Paraje El Pozo, (3000) Santa Fe, Argentina, http://www.cimec.org.ar*

[b]*Instituto de Ciências Matemáticas e de Computação (ICMC), USP, Av. do Trabalhador Sãocarlense 400, Centro, CEP 13560-970, São Carlos, SP, Brasil, http://www.icmc.usp.br*

Keywords: Oil Water Separation, Multiphase Flow, Algebraic Slip Mixture Model, Population Balance Equations, Hyperbolic Systems

Abstract. We discuss a model derived from the Williams population balance equations, written in mixture form, to represent water-in-oil emulsions undergoing separation by gravity. The model includes the treatment of the disperse phase, represented by a discrete distribution function at each material point, leading to the solution of the Population Balance Equations. This approach allows for a better representation of the physics of emulsions, providing a general framework to include phenomena such as inter-drop coalescence, coalescence with the homophase and the presence of dense-packed layers. The goal is to devise a solver for the complete system of equations (including momentum and mass conservation), so as to push forward the state of the art in the area, which nowadays relies mainly on one-dimensional kinematic separation models. Such an advanced solver is necessary to model the complete flow within separators of arbitrary geometries. This work includes a first description and discussion of the polydisperse model and the selection of a fast and accurate method for the solution of the system of one dimensional hyperbolic equations resulting from the treatment of the disperse phase.

1 INTRODUCTION

The presence of water in crude oil extraction has always been a part of the petroleum industry. The water plays the role of a passive component of the obtained mixture in case of new oil wells or has the objective of pressurization in the Enhanced Oil Recovery techniques. The emulsification of both fluids is the natural consequence of the presence of surfactants in the oil composition such as resins or asphaltenes. In addition, the components are intimately mixed by flowing through the porous structure of the reservoir and by the shear stresses due to the action of valves, pumps and other equipment present in the upstream (Frising et al., 2006).

Separation of water and oil is required mainly for reasons of product quality and water reuse. This is achieved by several methods being the gravity settlers the least expensive and simplest one. The physical mechanisms involved in these separation units have been studied using different approaches, including careful observation and interpretation of experiments. Barnea and Mizrahi (1975a,b,c,d), in a series of four seminal papers, gave a first systematic explanation of the process of gravity-induced liquid-liquid separation. The authors identify a dispersion layer within the settlers, composed of two sub-layers: a dense-packed layer and an even or sedimentation layer. The latter corresponds to a layer in which the droplets of the disperse phase are highly mobile, with some probability of growth in size by binary coalescence, depending on the local volume fraction. The settling droplets leave the sedimentation layer when they reach the dense-packed layer, where droplets eventually coalesce with their homo-phase (see Figure 1).

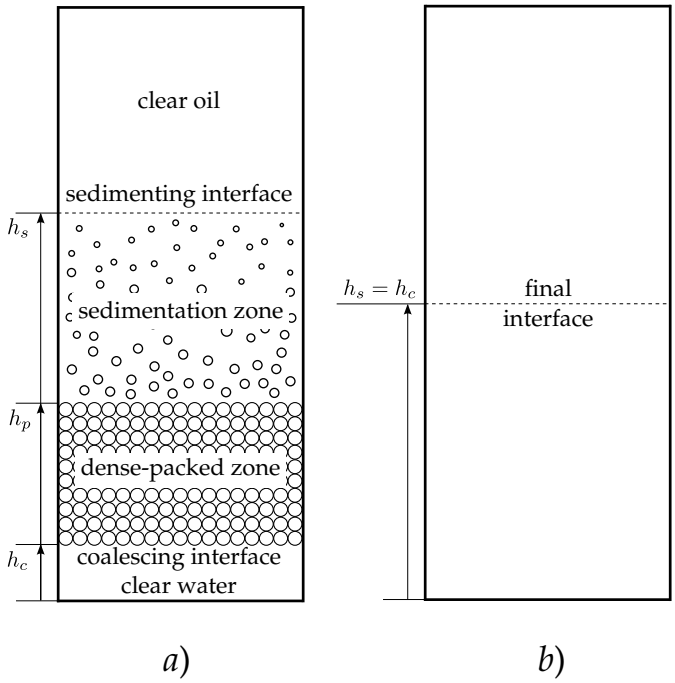

Figure 1: Scheme of batch settler and the evolution of the different front present within it. a) transient, b) final settled state.

Hartland and co-workers (Jeelani and Hartland, 1998, 1986; Hartland and Jeelani, 1987) gave important insights in the phenomenon of liquid-liquid separation, making the role of droplet size evolution within the dispersion layer clear and relating the batch laboratory experiments to more

real steady-state devices. They discussed the dynamics of the dense-packed layer, showing that it grows until a critical point at which sedimentation ends (when in batch configuration). After that, the system evolves only by drainage and coalescence with the homo-phase reaching the complete settled state. As a result of their studies they presented models for the kinematics of the coalescing and sedimentation fronts as well as the height of the dense-packed layer. Such models are based on experimental parameters such as the settling time, the initial dispersed phase diameter and the single-drop coalescing time.

Other authors presented similar models based on different parameters. In the work of Nadiv and Semiat (1995) they are the coalescence velocity and the sedimentation velocity. The work of Henschke et al. (2002) presents the most elaborate model to date, which addresses the droplet sedimentation, the evolution of the height of the dense-packed zone and the droplet deformation in the dense phase. In addition they introduce a coalescence equation containing the only free parameter of the model. Recent similar models, applied specifically to water-petroleum mixtures, can be found in the work of Frising et al. (2008) and Noïk et al. (2013). All these approaches can be classified as phenomenological models based on experimental data. Many assumptions are made which are inspired on basic research on the coalescence dynamics of two-drop systems. Related to this is the work Polderman and Bouma (1997), which puts forward general design rules on the sole basis of the Stokes law for droplet dynamics and a series of characteristic experiments. These rules set a basis for the dimensioning of industrial facilities, which can eventually be improved by using Hartland or Henschke models.

As was stated, the phenomenological models are based on knowledge obtained from experiments and/or theoretical estimates of the coalescing process. This process consists of drop-to-drop interaction/collision, drainage of the interfacial film subject to drop deformation, rupture of the film due to van der Waals and other intermolecular forces and to the presence of thermal and mechanical stresses (Palermo, 1991), and the redistribution after rupture of the surfactant and impurity concentration.

The state of the art within the branch of chemistry of dispersions is mostly represented by phenomenological models which describe the evolution of the different fronts present in batch settlers (front kinematics based models). A second phenomenological approach can be devised focused on the solution of the conservation equations which govern the problem. Recents works (Cunha et al., 2008; Grimes, 2012; Grimes et al., 2012) summarize the efforts in this topic and add new models and experimental validation based on Population Balance Equations (PBEs) models (Ramkrishna, 2000; Yeoh et al., 2014). The use of PBEs represents a general framework for the treatment of liquid-liquid dispersions respect to the conservervation of mass of the dispersed phase, which is considered as polydisperse. The solution of the PBEs gives the distribution of droplet volume for each material point of the separator. The discretization of these equations respect to the external coordinates (space) is done using standard discrezation techniques. On the other hand, the discretization of the distribution itself respect to the internal coordinates (volume and other physical parameters) is faced either by point, constant or linear approximations or the application of specific approaches such as Quadrature Moments Methods (QMOM) (Yeoh et al., 2014). Here it is important to remark that, the cited works are related to batch settlers with 1D approximations, which implies no solution for the flow of the continuous phase.

Then, an extension of the PBE approach is the coupling of PBE for the conservation of mass of the dispersed phase and a flow solver for the continuous phase. The works of Drumm (Drumm, 2010; Drumm et al., 2009) set a reference for this approach in the field of liquid-liquid separation. Here the mass conservation of the dispersed phase is solved via the PBE, then a momentum conservation equation is solved for the continuous and dispersed phase as is done in the two-fluids method (Drew and Passman, 1999). The momentum transfer between phases is managed using a drag law calculated with a representative diameter for the dispersed phase (Sauter diameter). A similar approach proposed in a more wide framework is given by Fevrier et al. (2005), there, the authors present the Mesoscopic Eulerian Formalism (MEF) which starts from the Williams-Boltzmann Equation (WBE) (Williams, 1958). This formalism considers a probability distribution function (PDF) not only dependent on droplet size but also in droplet velocity. It allows for writing both mass and momentum conservation equation in terms of PDF's. A complete generalization is presented by Vié (Vié et al., 2013; Vié, 2010) through the Multifluid Mesoscopic Eulerian Formalism (MMEF). Here the droplet population is divided in clasess, with its own momentum and mass conservation equations written in terms of PDF's. Then, the effect on the continuous phase is taken into account by an integrated drag term.

2 THEORETICAL FOUNDATION

Following the guidelines given by the MMEF the objective is to obtain a general mixture model suitable to be coupled with the PBE. Let the behavior of the dispersed phase be described by a PDF $f\left(\vec{x},\vec{v},V,t\right)$, where f is the probability that a particle located in $\vec{x}$ at time t had a volume V and velocity $\vec{v}$. This PDF is governed by the WBE as it is presented in Eqn. (1)

$$\frac{\partial f}{\partial t}+\vec{\nabla}_{\vec{x}}\cdot\left(\vec{v}\,f\right)+\vec{\nabla}_{\vec{v}}\cdot\left(\frac{\vec{F}_d}{m}\,f\right)=0 \tag{1}$$

Now it is worthy to define the following averages. The ensemble average for a quantity q, as in Eqn. (2)

$$\overline{q}=\int q\,f\left(\vec{x},\vec{v},V,t\right)\,d\vec{v}dV \tag{2}$$

and the mass-weighted average (Favre)

$$\hat{q}=\frac{1}{\overline{\rho}}\int m\,q\,f\left(\vec{x},\vec{v},V,t\right)\,d\vec{v}dV \tag{3}$$

where m is the mass of a single particle and $\overline{\rho}$ is the partial density defined as the ensemble average of the mass particles of the dispersed phase, as it is shown in Eqn. (4)

$$\overline{\rho}=\int m\,f\left(\vec{x},\vec{v},V,t\right)\,d\vec{v}dV \tag{4}$$

Therefore, multiplying Eqn. (1) by m and $m\,\vec{v}$ and integrating in $\vec{v}$ in a class of V_i+dV the mass and momentum conservation equations for class i are obtained as it is shown in Eqn. (5)

$$\begin{cases} \frac{\partial \overline{\rho}_i}{\partial t} + \vec{\nabla} \cdot \left(\overline{\rho}_i \, \hat{\vec{v}}_i \right) = 0 \\ \frac{\partial \overline{\rho}_i \, \hat{\vec{v}}_i}{\partial t} + \vec{\nabla} \cdot \left(\overline{\rho}_i \hat{\vec{v}}_i \otimes \hat{\vec{v}}_i \right) = \int \vec{F}_d \cdot \left(\vec{v} \otimes \vec{\nabla}_{\vec{v}} f \right) d\vec{v} - \vec{\nabla} \cdot \left(\frac{1}{3} \overline{\rho}_i \widehat{|\vec{w}|^2} - \overline{\rho}_i \widehat{\vec{w} \otimes \vec{w}} \right) \end{cases} \tag{5}$$

where $\vec{F}_{d,i}$ is the drag force over class i due to the interaction with the continuous phase. Now, due to the integration was done in each phase and the density was defined as a *partial* density, the extension for the whole domain implies the use of phase fractions, α_i (Drew and Passman, 1999), as it is presented in Eqn. (6)

$$\begin{cases} \frac{\partial \alpha_{w,i} \rho_{w,i}}{\partial t} + \vec{\nabla} \cdot \left(\alpha_{w,i} \rho_{w,i} \, \hat{\vec{v}}_{w,i} \right) = 0 \\ \frac{\partial \alpha_{w,i} \rho_{w,i} \, \hat{\vec{v}}_{w,i}}{\partial t} + \vec{\nabla} \cdot \left(\alpha_{w,i} \, \rho_{w,i} \hat{\vec{v}}_{w,i} \otimes \hat{\vec{v}}_{w,i} \right) = \int \vec{F}_d \cdot \left(\vec{v} \otimes \vec{\nabla}_{\vec{v}} f \right) d\vec{v} \\ \qquad\qquad - \vec{\nabla} \cdot \left(\frac{1}{3} \alpha_{w,i} \rho_{w,i} \widehat{|\vec{w}|^2} - \alpha_{w,i} \rho \widehat{\vec{w} \otimes \vec{w}} \right) \end{cases} \tag{6}$$

where the subscript w indicate the water phase. The conservation equations for the continuous phase follow the standard multi-fluid form, as in Eqn. (7)

$$\begin{cases} \frac{\partial \alpha_p \rho_p}{\partial t} + \vec{\nabla} \cdot \left(\alpha_p \rho_p \, \vec{v}_p \right) = 0 \\ \frac{\partial \alpha_p \rho_p \, \vec{v}_p}{\partial t} + \vec{\nabla} \cdot \left(\alpha_p \rho_p \vec{v}_p \otimes \vec{v}_p \right) = -\alpha_p \vec{\nabla} p_p + \vec{\nabla} \cdot \left(\alpha_p \overline{\overline{\tau_p}} \right) - \int \vec{F}_d \cdot \left(\vec{v} \otimes \vec{\nabla}_{\vec{v}} f \right) d\vec{v} \, dV \end{cases} \tag{7}$$

the last term is due to momentum exchange between petroleum and water phases taking into account the polydispersity of the water phase. The volume fractions for petroleum and water are such that $\alpha_p + \int \alpha_w(V) \, dV = 1$. Summing up both the momentum and mass conservation equations it is possible to obtain a simplified mixture formulation (Buscaglia et al., 2002) presented in Eqn. (8)

$$\begin{cases} \frac{\partial \rho_m}{\partial t} + \vec{\nabla} \cdot \left(\rho_m \, \vec{v}_m \right) = 0 \\ \frac{\partial \rho_m \, \vec{v}_m}{\partial t} + \vec{\nabla} \cdot \left(\rho_m \vec{v}_m \otimes \vec{v}_m \right) = -\vec{\nabla} p_m + \vec{\nabla} \cdot \left(\overline{\overline{\tau_m}} \right) - \vec{\nabla} \cdot \left[\int \alpha_w(V) \rho_w(V) \, \vec{v}_{wp} \otimes \vec{v}_{wp} \, dV \right] \end{cases} \tag{8}$$

where $\rho_m = \alpha_p \rho_p + \overline{\rho}_w$ is the mixture density, $\vec{v}_m = (\alpha_p \rho_p \vec{v}_p + \hat{\vec{v}}_w)/\rho_m$ is the center-of-mass velocity and $\vec{v}_{wp}$ is the relative velocity of water (dispersed) phase for each droplet size respect to the petroleum (continuous phase). In addition, an expression for $\overline{\overline{\tau_m}}$ is needed. The solution of the system also requires to know the distribution of phases, which is achieved by the solution of the mass conservation equation for each class. In the particular case of class i [first equation in Eqn.(6)] it reads as in Eqn. (9).

$$\frac{\partial \alpha_{w,i}}{\partial t} + \vec{\nabla} \cdot \left(\alpha_{w,i} \, \hat{\vec{v}}_{w,i} \right) = 0 \tag{9}$$

The mass conservation equation for the mixture can be simplified using a center-of-volume velocity $\vec{u} = \alpha_p \vec{v}_p + \int \alpha_w(V)\vec{v}_w(V)\, dV$ leading to the system in Eqn. (10) (Manninen et al., 1996; Márquez Damián, 2013; Márquez Damián and Nigro, 2014).

$$\begin{cases} \vec{\nabla} \cdot \vec{u} = 0 \\ \frac{\partial \rho_m \vec{v}_m}{\partial t} + \vec{\nabla} \cdot (\rho_m \vec{v}_m \otimes \vec{v}_m) = -\vec{\nabla} p_m + \vec{\nabla} \cdot \left(\overline{\overline{\tau_m}}\right) - \vec{\nabla} \cdot \left[\int \alpha_w(V)\rho_w(V)\, \vec{v}_{wp} \otimes \vec{v}_{wp}\, dV\right] \\ \frac{\partial \alpha_{w,i}}{\partial t} + \vec{\nabla} \cdot (\alpha_{w,i}\, \vec{u}) + \vec{\nabla} \cdot (\alpha_{w,i}\, \vec{v}_{dr,wi}) = 0 \end{cases} \tag{10}$$

where it is necessary to solve as many mass conservation equations as classes were selected. This system has the great advantage to have a divergence free velocity which simplifies the pressure-velocity coupling resolution and the integration of the mass conservation equation for $\alpha_{w,i}$. The distribution of each phase is known by solving the mass conservation equation for a class i [third equation in Eqn.(10)] as it is presented in Eqn. (11).

$$\frac{\partial \alpha_{w,i}}{\partial t} + \vec{\nabla} \cdot (\alpha_{w,i}\, \vec{u}) + \vec{\nabla} \cdot (\alpha_{w,i}\, \vec{v}_{dr,wi}) = 0 \tag{11}$$

where $\vec{v}_{dr,wi} = \vec{v}_{w,i} - \vec{v}_m$ is a relative velocity between the dispersed phase and the center-of-volume and can be calculated as it is Eqn. (12)

$$\vec{v}_{dr,wi} = \vec{v}_{wp,i}\,(1 - \alpha_{w,i}) - \sum_{j \neq i}^{N} \alpha_{w,j}\, \vec{v}_{wp,j} \tag{12}$$

where N is the number of classes used for the discretization of the problem. The closure of such a model involves the determination of relative velocity, $\vec{v}_{wp}$, which in principle requires the solution of each one of the disperse phase momentum equations [second expression in Eqn. (5)] and thus the knowledge of mometum exchange terms, for which no closed formula is available.

Another possibility is to plug into Eqn. (12) an expression for $\vec{v}_{wp}$ based on experimental evidence and/or micro-mechanical models. Frising et al. (2008), for example, proposed an expression based on their experiments which is presented in Eqn. (13)

$$\vec{v}_{wp,i} = V_0\ (1 - \alpha_{w,i})^6 \tag{13}$$

where V_0 is the velocity of a single droplet.

2.1 One dimensional problem reduction

For one dimensional batch problems it is easy to prove that $\vec{u} = 0$ and the solution of the problem reduces to the integration of the dispersed phase mass conservation equations which are simplified to Eqn. (14)

$$\frac{\partial \alpha_{w,i}}{\partial t} + \vec{\nabla} \cdot \left\{ \alpha_{w,i} \left[\vec{v}_{wp,i}\,(1 - \alpha_{w,i}) - \sum_{j \neq i}^{N} \alpha_{w,j}\, \vec{v}_{wp,j} \right] \right\} = 0 \tag{14}$$

This equation allows to know the distribution of phases within the settler and the evolution of the fronts discussed in the previous models. The fronts are solved as traveling shock waves, while the smooth transitions constitute traveling rarefaction fans (Bürger et al., 2008). This equation has a flux function given by Eqn. (15)

$$\mathrm{F}(\alpha_{w,i}) = \alpha_{w,i}\left[\vec{v}_{wp,i}\,(1-\alpha_{w,i}) - \sum_{j\neq i}^{N}\alpha_{w,j}\,\vec{v}_{wp,j}\right] \tag{15}$$

where it is again necessary to define an expression for the relative velocity, $\vec{v}_{wp,i}$. Following the concepts presented in the last section it is possible to define a law for the relative velocity such as presented in Eqn. (16)

$$\vec{v}_{wp,i} = \vec{v}_{0,i}\,\left(\beta_{\max} - \beta_w\right)^{a_i} \tag{16}$$

where $\beta_w = \sum_{i=1}^{N}\alpha_{w,i}$, is the total phase fraction of water in each point and $\beta_{\max}$ is the maximum allowable water phase fraction before coalescence with homophase, or in other words, the phase fraction of the dense-packed layer. Here it is important to remark that the velocity laws must include β_w instead of each class water phase fraction, since the combined effect of water droplets of different sizes determines the possibility of drop sedimentation.

3 NUMERICAL METHODS

In order to integrate the system of N transport equations which governs the evolution of the PDF for the water dispersed phase an explicit method will be used as it is shown in Eqn. (17)

$$\alpha_{w,i}^{n+1} = \alpha_{w,i}^{n} - \frac{\Delta t}{V_k}\sum_{f}\left\{\left[\vec{v}_{wp,i}\left(1-\alpha_{w,i}^{n}\right) - \sum_{j\neq i}^{N}\alpha_{w,j}^{n}\,\vec{v}_{wp,j}\right]\alpha_{w,i}^{n}\right\}_{f}\cdot\vec{S}_f \tag{17}$$

where n is the time-step index, f is the face index, V_k is the volume of the k-th cell and $\vec{S}_f$ face area normal. The implementation using the OpenFOAM® suite (Weller et al., 1998) is based on the decomposition given in Eqn. (18)

$$\alpha_{w,i}^{n+1} = \alpha_{w,i}^{n} - \frac{\Delta t}{V_k}\sum_{f}\left\{\left[\vec{v}_{wp,i}\left(1-\alpha_{w,i}^{n}\right)\right]\left(\alpha_{w,i}^{n}\right)_a - \left[\sum_{j\neq i}^{N}\alpha_{w,j}^{n}\,\vec{v}_{wp,j}\right]\left(\alpha_{w,i}^{n}\right)_b\right\}_{f}\cdot\vec{S}_f \tag{18}$$

which can be rewritten as in Eqn. (19),

$$\alpha_{w,i}^{n+1} = \alpha_{w,i}^{n} - \frac{\Delta t}{V_k}\sum_{f}\left\{\vec{v}_{a,i}\left(\alpha_{w,i}^{n}\right)_a - \vec{v}_{b,i}\left(\alpha_{w,i}^{n}\right)_b\right\}_{f}\cdot\vec{S}_f \tag{19}$$

Here the advective nature of the system is very clear, with two advection velocities: $\vec{v}_{a,i}$ or the own class relative velocity and $\vec{v}_{b,i}$ which takes into account the effect of all other classes. The transported variable $\alpha_{w,i}$ is separated in two different entities, $(\alpha_{w,i}^{n})_a$ and $(\alpha_{w,i}^{n})_b$, in order to allow for different face interpolation of each one. The values of $\alpha_{w,i}^{n}$ for the calculation of the relative velocities, $\vec{v}_{a,i}$ and $\vec{v}_{b,i}$ are always interpolated linearly. It is important to remark that in this method the face values of the advected quantities are calculated based only on the information given by the relative velocities and no information about the eigenstructure of the

hyperbolic system is used.

In addition, four other schemes specially tailored for hyperbolic problems, are used in order to select the most suitable one for the integration of the system, namely: Lax-Friederichs (LxF), Rusanov, Roe (Toro, 2009; LeVeque, 2002) and Kurganov and Tadmor (KT) (Kurganov and Tadmor, 2000). The LxF scheme is known as a simple method for the integration of a system of hyberbolic equations, however, its main drawback is the excessive numerical diffusion introduced. Even though, using fine meshes and small time-steps reference solutions can be obtained easily. All of these schemes, for the one dimensional case, can be written in the compact form presented in Eqn. (20)

$$\alpha^{n+1}_{w,i,k} = \alpha^{n}_{w,i.k} - \frac{\Delta t}{\Delta x}\left[\tilde{\mathrm{F}}(\alpha_{w,i,k+1/2}) - \tilde{\mathrm{F}}(\alpha_{w,i,k-1/2})\right] \tag{20}$$

which gives the solution for the phase fraction of class i in cell k. Here $\tilde{\mathrm{F}}$ are numerically stabilized fluxes which are given at the $k+1/2$ and $k-1/2$ interfaces. i.e. the left and right interfaces of the k-th cell. Therefore, the following fluxes are defined:

Lax-Friederichs

$$\tilde{\mathrm{F}}^{\mathrm{LxF}} = \frac{\mathrm{F}\left(\alpha^{n}_{w,i,+}\right) + \mathrm{F}\left(\alpha^{n}_{w,i,-}\right)}{2} - \frac{1}{2}\frac{\Delta x}{\Delta t}\left(\alpha^{n}_{w,i,+} - \alpha^{n}_{w,i,-}\right) \tag{21}$$

Rusanov

$$\tilde{\mathrm{F}}^{\mathrm{Rus}} = \frac{\mathrm{F}\left(\alpha^{n}_{w,i,+}\right) + \mathrm{F}\left(\alpha^{n}_{w,i,-}\right)}{2} - \frac{1}{2}\lambda^{\max}\left(\alpha^{n}_{w,i,+} - \alpha^{n}_{w,i,-}\right) \tag{22}$$

Roe

$$\tilde{\mathrm{F}}^{\mathrm{Roe}} = \frac{\mathrm{F}\left(\alpha^{n}_{w,i,+}\right) + \mathrm{F}\left(\alpha^{n}_{w,i,-}\right)}{2} - \frac{1}{2}\sum_{m} r^{m}\left|\lambda^{m}\right| l^{m}\left(\alpha^{n}_{w,i,+} - \alpha^{n}_{w,i,-}\right) \tag{23}$$

Kurganov and Tadmor

$$\tilde{\mathrm{F}}^{\mathrm{KT}} = \frac{\mathrm{F}\left(\alpha^{n}_{w,i,+}\right) + \mathrm{F}\left(\alpha^{n}_{w,i,-}\right)}{2} - \frac{1}{2}a\left(\alpha^{n}_{w,i,+} - \alpha^{n}_{w,i,-}\right) \tag{24}$$

where $\alpha^{n}_{w,i,-}$ and $\alpha^{n}_{w,i,+}$ represent the values of $\alpha^{n}_{w,i}$ at left and right sides of a given interface, F is the flux defined in Eqn. (15), λ^{m} is the m-th of the N eigenvalues of the jacobian matrix for the flux $A = \frac{\partial \mathrm{F}}{\partial \alpha_{w,i}}$, used for the linearization of the problem. In addition, r^{m} and l^{m} are the corresponding right and left eigenvalues, $\lambda^{\max}$ is the maximum eigenvalue and a is the maximum of spectral radius evaluated at left and right sides of the interface. The Rusanov and Roe fluxes require only one jacobian evaluation at each interface which is done using the Roe's mean as the argument. For the sake of simplicity the value of the Roe's mean is taken as $\alpha^{\mathrm{Roe}}_{w,i} = (\alpha_{w,i,-} + \alpha_{w,i,+})/2$. In the case of the KT scheme the jacobian is evaluated at both sides of the interface. It is important to remark that in Rusanov and Roe fluxes the values of $\alpha_{w,i}$ are considered to be constant, in KT scheme the values at $\alpha_{w,i,-}$ and $\alpha_{w,i,+}$ at interfaces are *reconstructed* from the cell center values using TVD functions (Sweby, 1984). Therefore, if constant reconstruction is used, KT and Rusanov fluxes are fairly similar.

4 NUMERICAL RESULTS

The schemes presented in the previous section are tested in a model sedimentation problem. It represents a one dimensional settler with height, $h = 1\,\mathrm{m}$. The system is filled with a mixture of petroleum and water, where the latter is divided in three classes, $\alpha_{w,1} = 0.1$, $\alpha_{w,2} = 0.15$ and $\alpha_{w,3} = 0.2$. Then, the petroleum phase has $\alpha_p = 0.55$. The relative velocity constants are $V_{0,1} = -0.5\frac{\mathrm{m}}{\mathrm{sec}}$, $V_{0,2} = -1\frac{\mathrm{m}}{\mathrm{sec}}$ and $V_{0,3} = -2\frac{\mathrm{m}}{\mathrm{sec}}$ while $a_i = 1$ in all cases. The water fraction for the dense-packed layer is set as $\beta_{\max} = 0.74$.

The scheme given in Eqn. (19) was implemented (Márquez Damián et al., 2012) using OpenFOAM® and the other four schemes using `octave-of` (Márquez Damián et al., 2012). The domain was discretized using 400 regular cells ($\Delta x = 0.0025\,\mathrm{m}$, base mesh), with $\Delta t = 0.001\,\mathrm{sec}$ and the calculations were done until $t = 1\,\mathrm{sec}$ and $t = 8\,\mathrm{sec}$. In addition, a reference solution was obtained for $t = 1\,\mathrm{sec}$ using 10,000 regular cells ($\Delta x = 0.0001\,\mathrm{m}$), with $\Delta t = 0.00004\,\mathrm{sec}$ and the LxF scheme.

Therefore, Figures 2-9 present the reference solution by LxF scheme and then solutions for OpenFOAM®, LxF, Rusanov, Roe and KT schemes for the base mesh at $t = 1\,\mathrm{sec}$. The thick continuous line represents the total water fraction, short dashed line $\alpha_{w,1}$, long dashed line $\alpha_{w,2}$, long and short dashed line $\alpha_{w,3}$ and continuous thin line the petroleum phase fraction. The case in OpenFOAM® was set such that $(\alpha^n_{w,i})_a$ has TVD Minmod reconstruction (Roe, 1986) and $(\alpha^n_{w,i})_b$ has linear reconstruction. In case of KT schemes these were tested using constant, Minmod and vanLeer (Van Leer, 1974) reconstructions. From the figures it is possible to affirm that the OpenFOAM® solution presents a good approximation to the reference case but exhibits excessive compression in rarefaction waves and the dense-packed layer value is exceeded. In the case of LxF in base mesh the solution is excessively diffusive. Then, solutions for Rusanov, Roe, KT-constant are similar and slightly more diffusive than the reference solution. Finally, the case of KT-Minmod presents excellent agreement and KT-vanLeer a little more compression than needed as it is shown in the rarefaction fans.

A second group of calculations, for $t = 8\,\mathrm{sec}$, is presented in Figures 11-16. There, the solution for OpenFOAM®, which was obtained using the reconstruction schemes selected in the previous case, presents wiggles and overshoots exceeding the the dense-packed layer value. All other schemes present bounded solutions. As is expected the LxF scheme gives an excessive diffusive solution. Rusanov and KT-constant are less diffusive but still not appropriate solutions. The best cases are those given by Roe, KT-Minmod and KT-van Leer schemes. Here it is important to remark that since at long times the system evolves only by shock waves, the preferable schemes result KT-van Leer or Roe.

5 CONCLUSIONS

In this work a mixture model for water-in-oil mixtures based on the Multifluid Mesoscopic Eulerian Formalism was presented. The discretization of the PDF related to the evolution of the dispersed phase requires the integration of a system of non-linear hyperbolic equations which has to be done fast and accurately.

Therefore, a series of tests were carried out in order to select an appropriate scheme for such

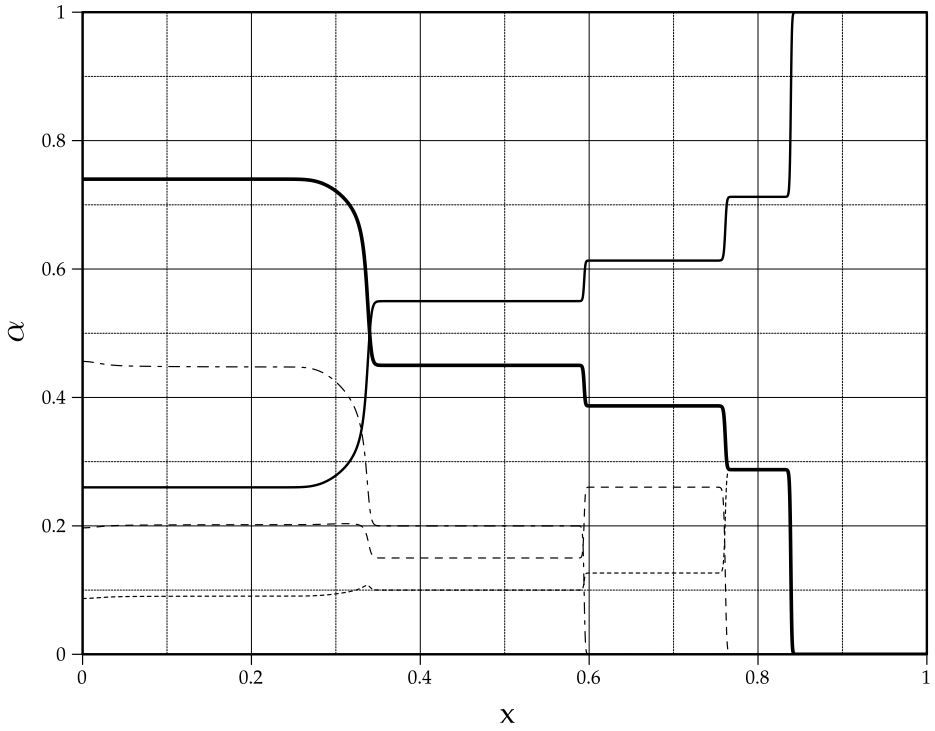

Figure 2: Solution by LxF scheme for reference mesh at $t = 1\,\mathrm{sec}$.

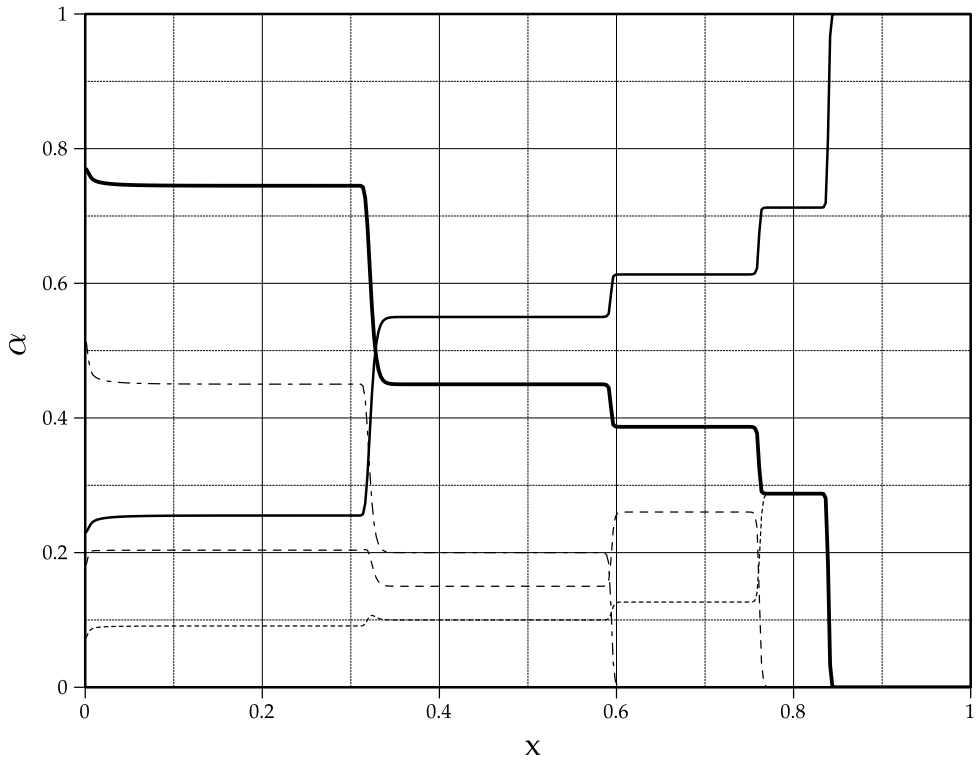

Figure 3: Solution using OpenFOAM® in base mesh at $t = 1\,\mathrm{sec}$.

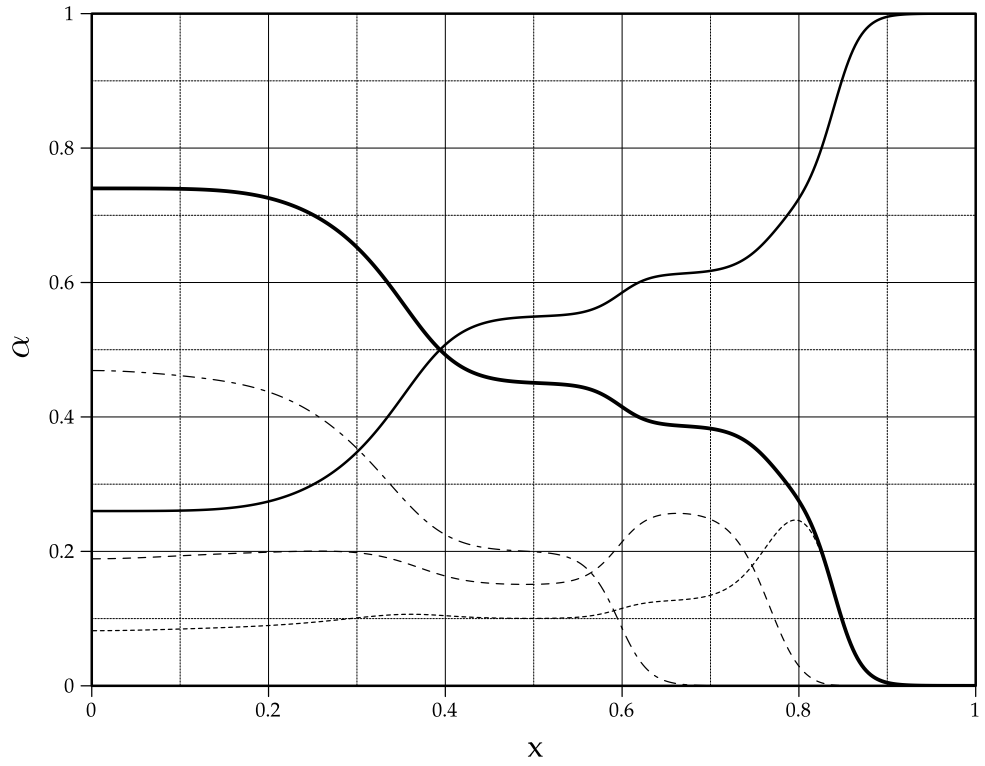

Figure 4: Solution by LxF scheme for base mesh at $t = 1\,\mathrm{sec}$.

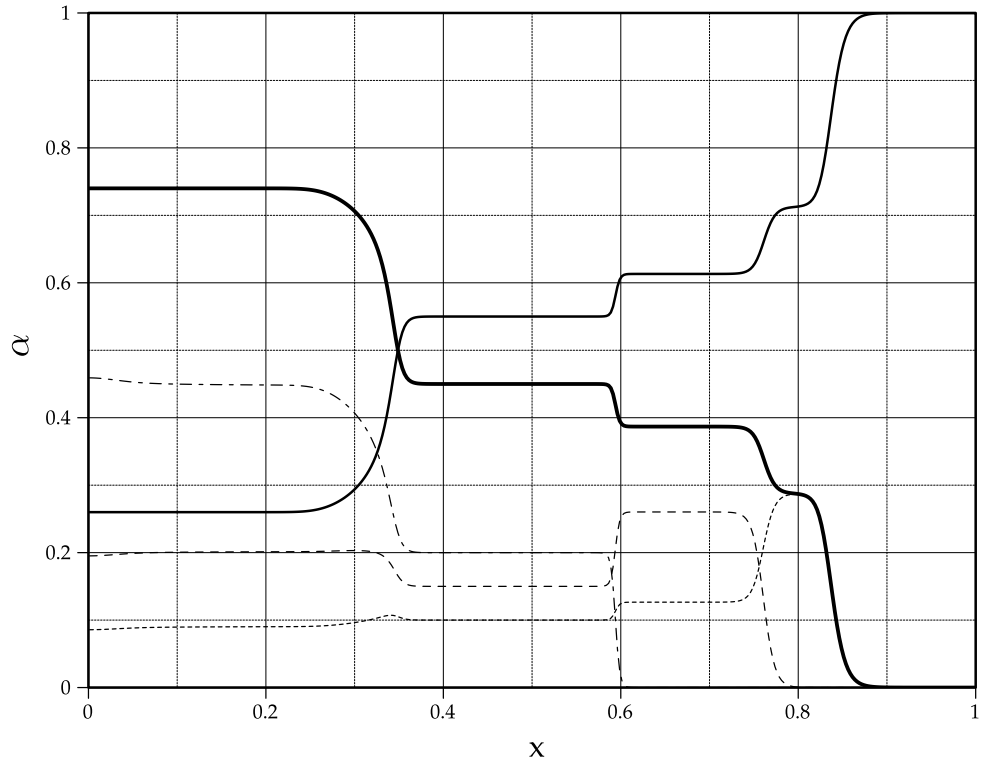

Figure 5: Solution by Rusanov scheme for base mesh at $t = 1\,\mathrm{sec}$.

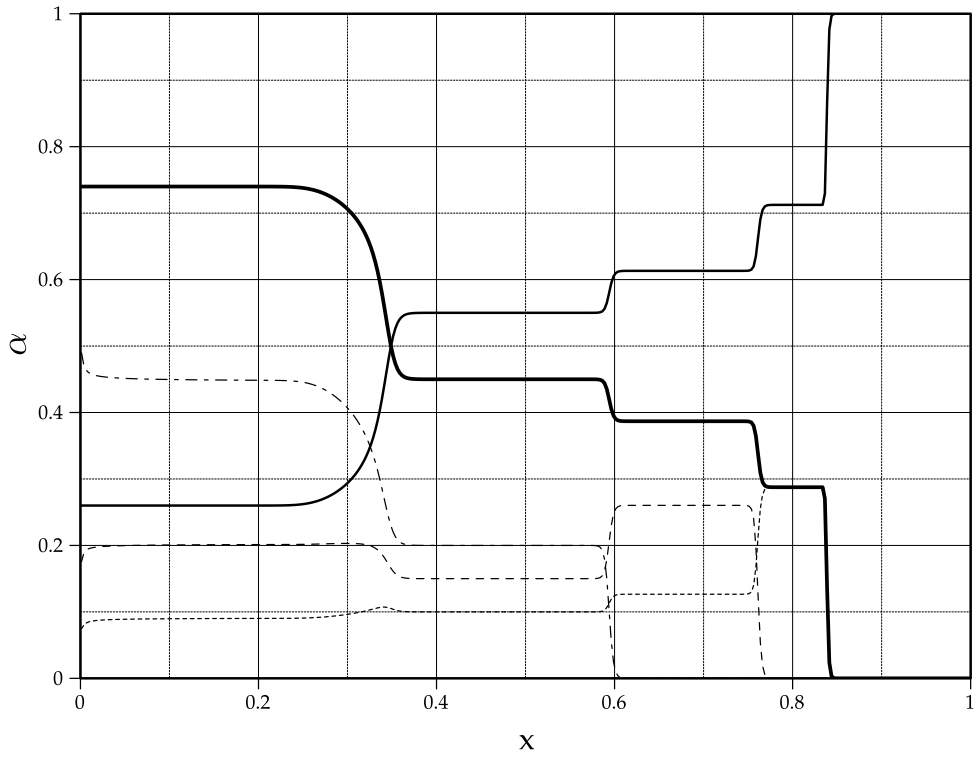

Figure 6: Solution by Roe scheme for base mesh at $t = 1\,\mathrm{sec}$.

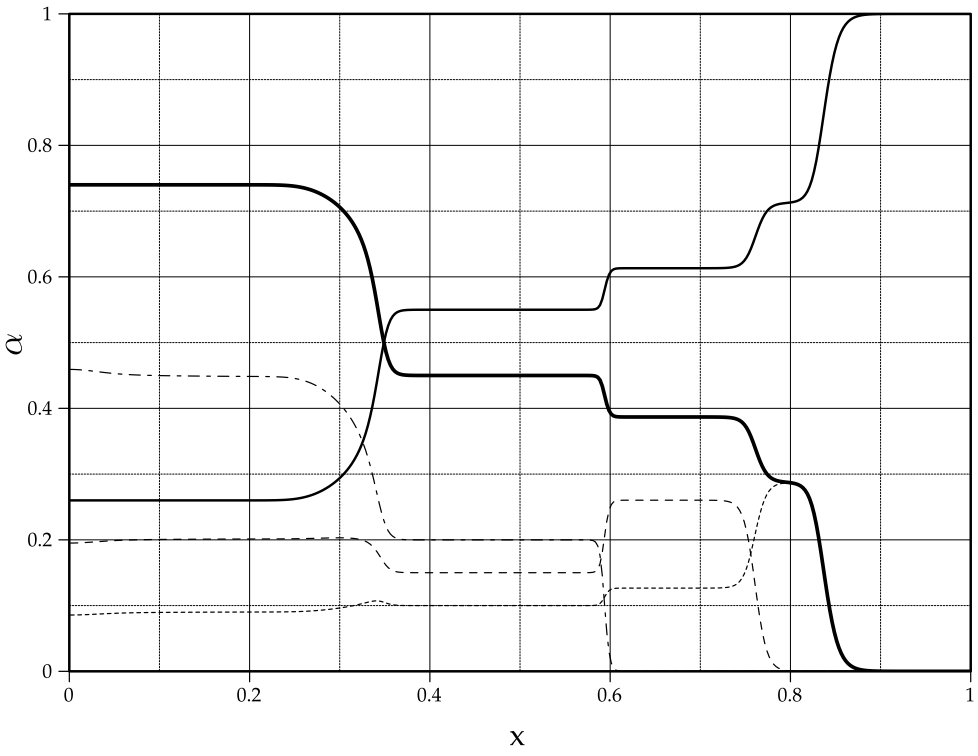

Figure 7: Solution by KT scheme with constant reconstruction for base mesh at $t = 1\,\mathrm{sec}$.

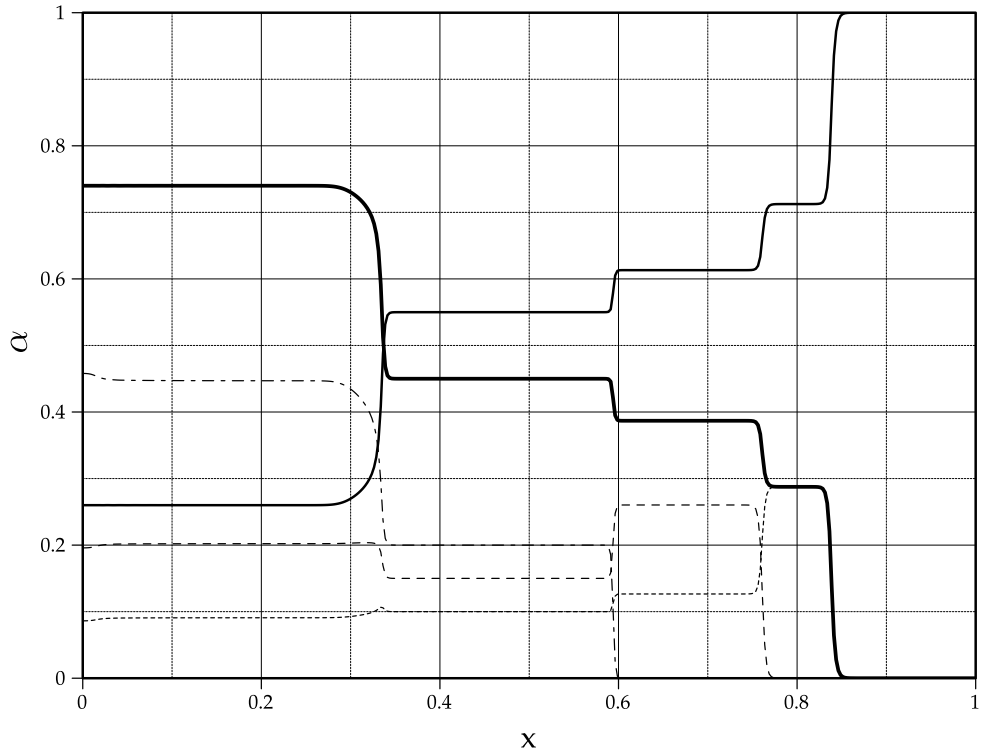

Figure 8: Solution by KT scheme with Minmod reconstruction for base mesh at $t = 1\,\mathrm{sec}$.

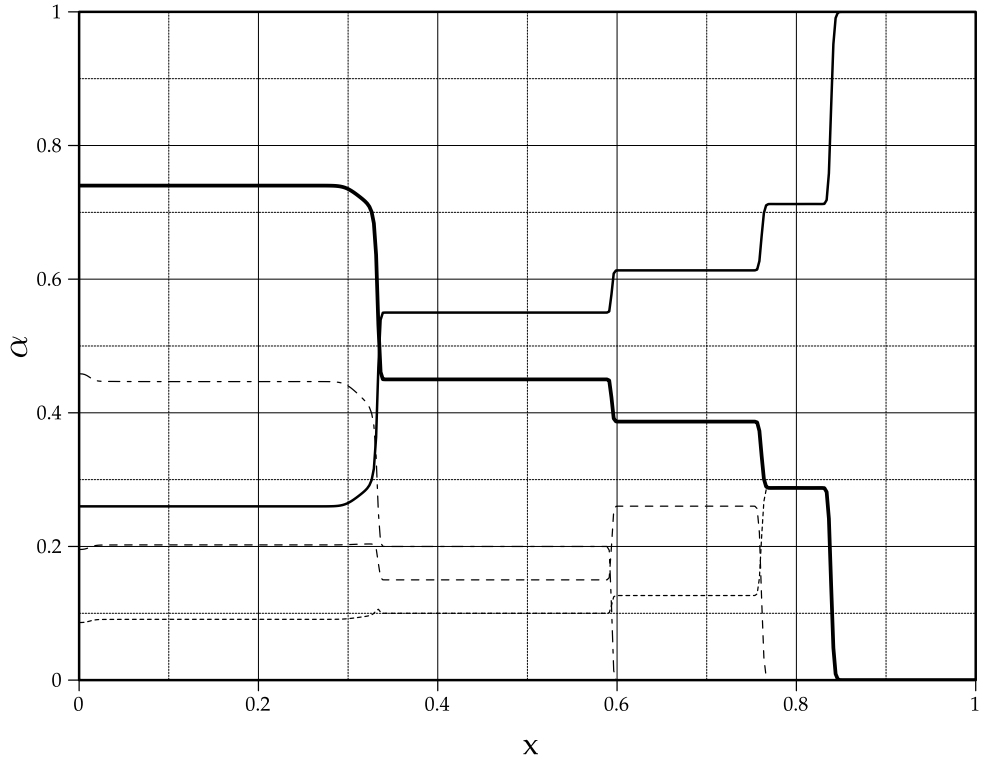

Figure 9: Solution by KT scheme with van Leer reconstruction for base mesh at $t = 1\,\mathrm{sec}$.

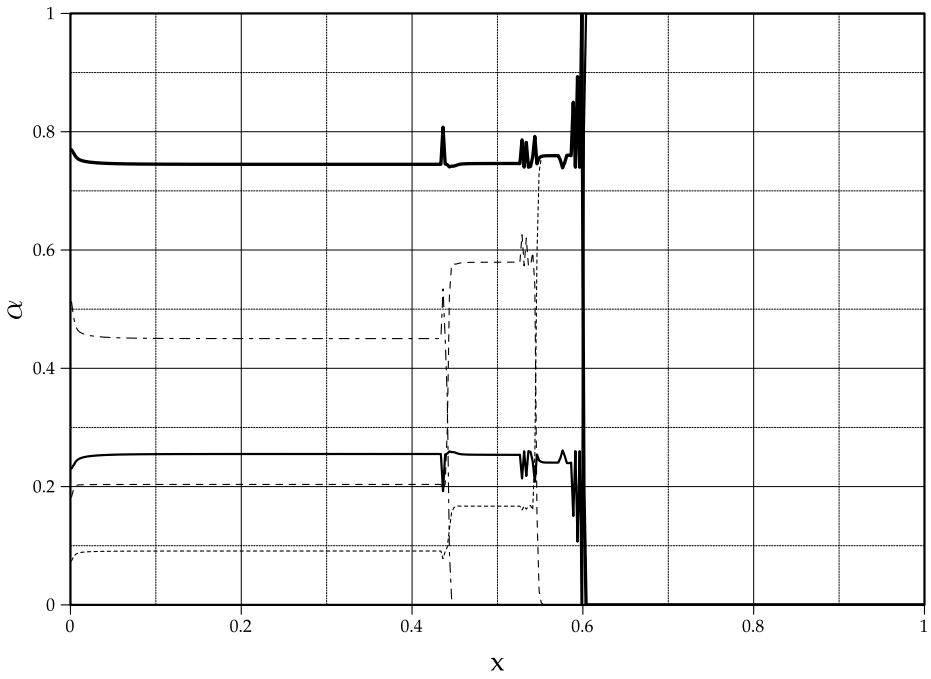

Figure 10: Solution using OpenFOAM® in base mesh at $t = 8\,\mathrm{sec}$.

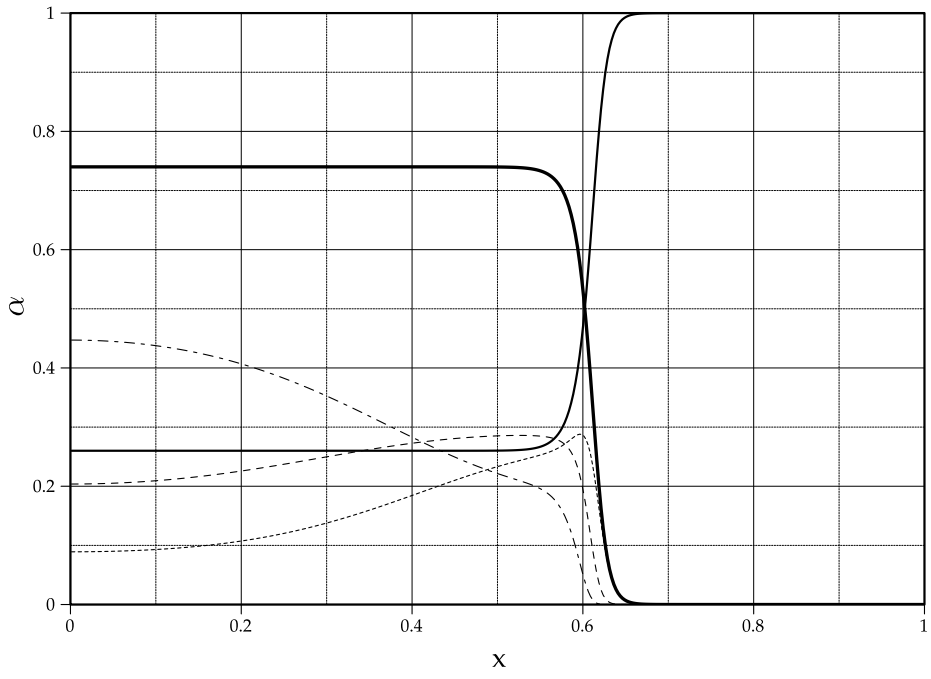

Figure 11: Solution by LxF scheme for base mesh at $t = 8\,\mathrm{sec}$.

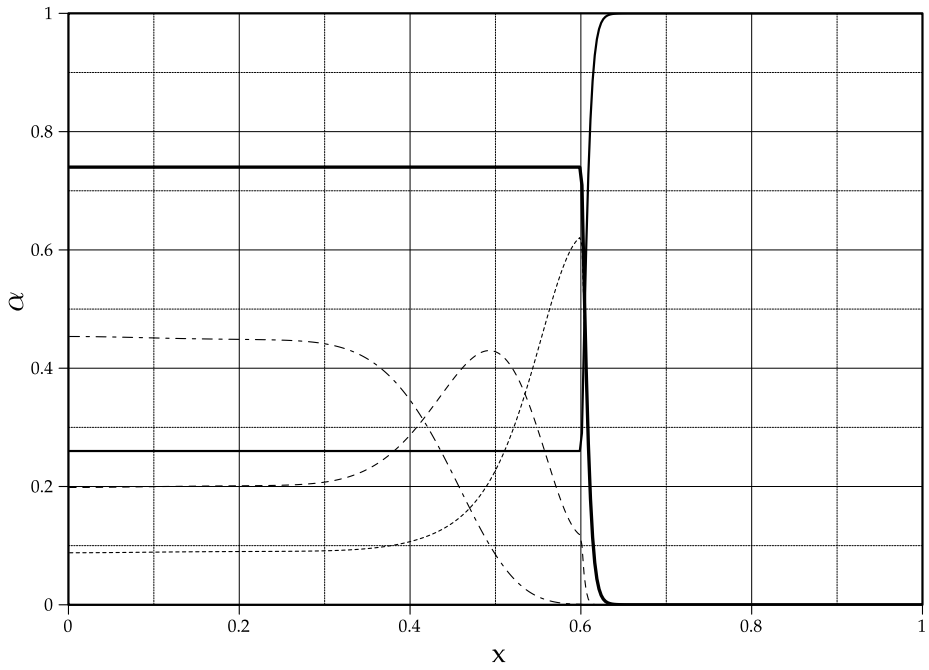

Figure 12: Solution by Rusanov scheme for base mesh at $t = 8\,\mathrm{sec}$.

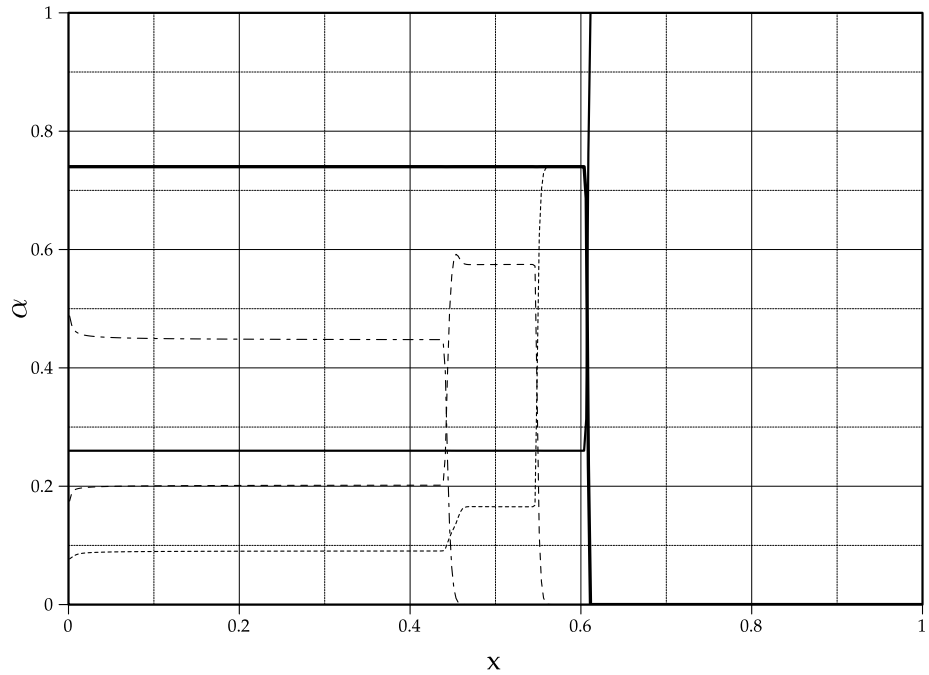

Figure 13: Solution by Roe scheme for base mesh at $t = 8\,\mathrm{sec}$.

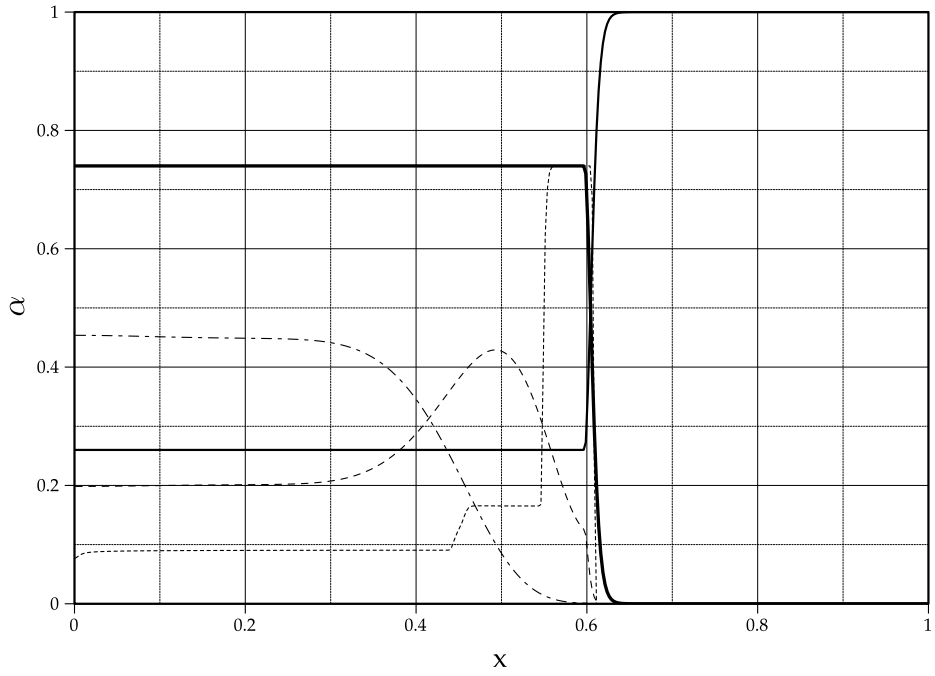

Figure 14: Solution by KT scheme with constant reconstruction for base mesh at $t = 8\,\mathrm{sec}$.

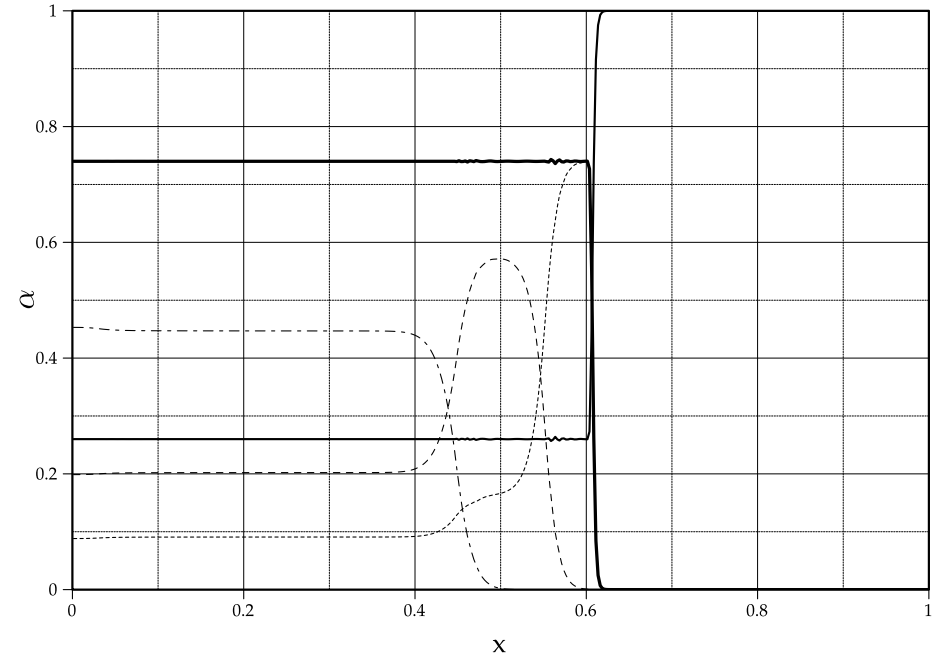

Figure 15: Solution by KT scheme with Minmod reconstruction for base mesh at $t = 8\,\mathrm{sec}$.

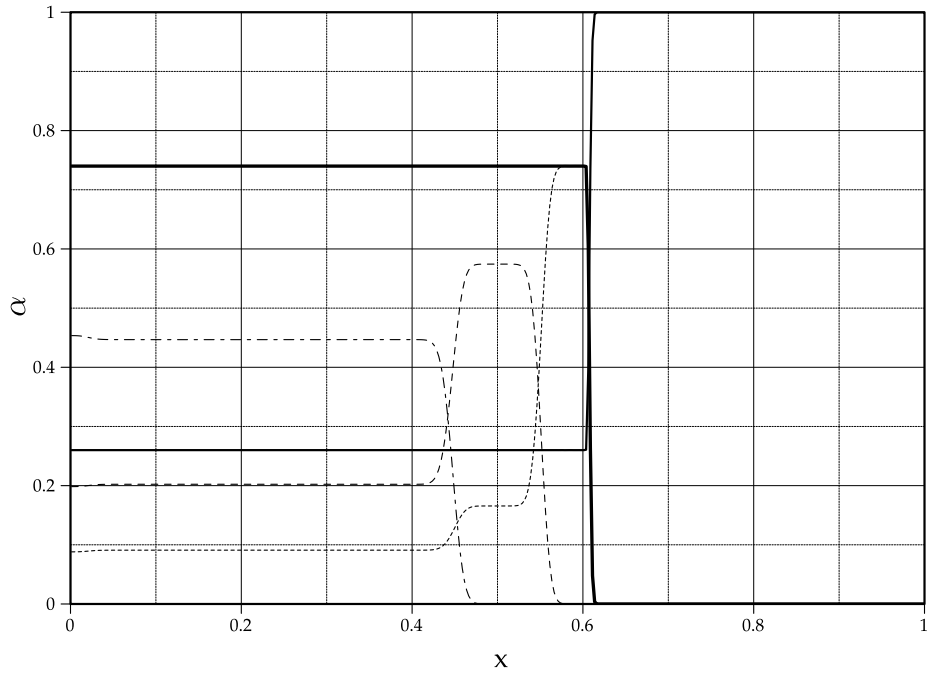

Figure 16: Solution by KT scheme with van Leer reconstruction for base mesh at $t = 8\,\mathrm{sec}$.

task. The Lax-Friedrichs scheme performed overdiffusively in all cases. The schemes of Rusanov and Kurganov and Tadmor with constant reconstruction showed better performance but still have too much diffusion for practical cases. The scheme implemented in OpenFOAM® was promissory at first stages but presented many spurious oscillations and the dense-packed phase fraction was not preserved. Its main advantage is to avoid the calculation of the flux jacobians and the associated eigenvalues and eigenvectors. The best results were obtained by the schemes of Roe and Kurganov and Tadmor with Minmod and van Leer reconstructions.

The method of Roe has a wide range of applicability giving accurate solutions at all times but requires the evaluation of eigenvalues and eigenvectors which is is huge task. On the other hand, Kurganov and Tadmor schemes are simple since they only require the evaluation of the spectral radius, this calculation can be simplified, for example, using the Gelfand's formula. The only drawback in this case is the necessity of calculate this value twice in each interface.

In view of the presented results the recommended scheme for Population Balance Equations integration is Kurganov and Tadmor with TVD reconstruction. The solution of these equations will be used as a basis for a coupled flux and phase-distribution solver capable to manage sedimentation problems in continuous regime and not only in batch cases.

6 ACKNOWLEDGEMENT

The authors wish to give thanks to Centro de Matemática e Estatística Aplicadas à Indústria (CePID-CeMEAI), FAPESP (grant N° 2012/14481-8), CONICET and Universidad Nacional del Litoral for their financial support.

An special acknowledgment is given to OpenFOAM®, gdb, octave, Inkscape and Paraview®

developers and users community for their contribution to free software.

REFERENCES

Barnea E. and Mizrahi J. Separation mechanism of liquid—liquid dispersions in a deep-layer gravity settler: Part I—The structure of the dispersed band. *Trans. Inst. Chem. Eng*, 53:61–69, 1975a.

Barnea E. and Mizrahi J. Separation mechanism of liquid–liquid dispersions in a deep-layer gravity settler: Part II—Flow patterns of the dispersed and continuous phases within the dispersion band. *Trans. Inst. Chem. Eng*, 53:70–74, 1975b.

Barnea E. and Mizrahi J. Separation mechanism of liquid–liquid dispersions in a deep-layer gravity settler: Part III—Hindered settling and drop-to-drop coalescence in the dispersion band. *Trans. Inst. Chem. Eng*, 53:75–82, 1975c.

Barnea E. and Mizrahi J. Separation mechanism of liquid–liquid dispersions in a deep-layer gravity settler: Part IV—Continuous settler characteristics. *Trans. Inst. Chem. Eng*, 53:83–92, 1975d.

Bürger R., García A., Karlsen K., and Towers J. A family of numerical schemes for kinematic flows with discontinuous flux. *Journal of Engineering Mathematics*, 60(3-4):387–425, 2008.

Buscaglia G., Bombardelli F., and Garcia M. Numerical modeling of large-scale bubble plumes accounting for mass transfer effects. *International Journal of Multiphase flow*, 28(11):1763–1785, 2002.

Cunha R., Fortuny M., Dariva C., and Santos A. Mathematical modeling of the destabilization of crude oil emulsions using population balance equation. *Industrial & Engineering Chemistry Research*, 47(18):7094–7103, 2008.

Drew D. and Passman S. *Theory of multicomponent fluids*. Springer Verlag, 1999.

Drumm C. *Coupling of computational fluid dynamics and population balance modelling for liquid-liquid extraction*. Ph.D. thesis, Technischen Universität Kaiserslautern, Kaiserslautern, 2010.

Drumm C., Attarakih M., and Bart H. Coupling of CFD with DPBM for an RDC extractor. *Chemical Engineering Science*, 64(4):721–732, 2009.

Fevrier P., Simonin O., and Squires K.D. Partitioning of particle velocities in gas–solid turbulent flows into a continuous field and a spatially uncorrelated random distribution: theoretical formalism and numerical study. *Journal of Fluid Mechanics*, 533:1–46, 2005.

Frising T., Noïk C., and Dalmazzone C. The liquid/liquid sedimentation process: from droplet coalescence to technologically enhanced water/oil emulsion gravity separators: a review. *Journal of Dispersion Science and Technology*, 27(7):1035–1057, 2006.

Frising T., Noïk C., Dalmazzone C., Peysson Y., and Palermo T. Contribution of the sedimentation and coalescence mechanisms to the separation of concentrated water-in-oil emulsions. *Journal of Dispersion Science and Technology*, 29(6):827–834, 2008.

Grimes B. Population balance model for batch gravity separation of crude oil and water emulsions. Part I: Model formulation. *Journal of Dispersion Science and Technology*, 33(4):578–590, 2012.

Grimes B., Dorao C., Opedal N., Kralova I., Sørland G., and Sjöblom J. Population balance model for batch gravity separation of crude oil and water emulsions. Part II: Comparison to experimental crude oil separation data. *Journal of Dispersion Science and Technology*, 33(4):591–598, 2012.

Hartland S. and Jeelani S. Choice of model for predicting the dispersion height in liquid/liquid gravity settlers from batch settling data. *Chemical Engineering Science*, 42(8):1927–1938,

1987.
Henschke M., Schlieper L., and Pfennig A. Determination of a coalescence parameter from batch-settling experiments. *Chemical Engineering Journal*, 85(2-3):369–378, 2002.
Jeelani S. and Hartland S. Variation of drop size and hold-up in a dense-packed dispersion. *Chemical Engineering and Processing: Process Intensification*, 20(5):271–276, 1986.
Jeelani S. and Hartland S. Effect of dispersion properties on the separation of batch liquid-liquid dispersions. *Industrial & engineering chemistry research*, 37(2):547–554, 1998.
Kurganov A. and Tadmor E. New high-resolution central schemes for nonlinear conservation laws and convection-diffusion equations. *Journal of Computational Physics*, 160(1):241–282, 2000.
LeVeque R. *Finite volume methods for hyperbolic problems*. Cambridge Univ Press, 2002.
Manninen M., Taivassalo V., and Kallio S. *On the mixture model for multiphase flow*. Technical Research Centre of Finland, Espoo, 1996.
Márquez Damián S. *An extended mixture model for the simultaneous treatment of short and long scale interfaces*. Ph.D. thesis, FICH, Universidad Nacional del Litoral, Santa Fe, Argentina, 2013.
Márquez Damián S., Corzo S., and Nigro N. octave-of Octave 1D emulator of OpenFOAM(R). http://http://code.google.com/p/octave-of/, 2012.
Márquez Damián S., Giménez J., and Nigro N. gdbOF: A debugging tool for OpenFOAM®. *Advances in Engineering Software*, 47(1):17–23, 2012.
Márquez Damián S. and Nigro N.M. An extended mixture model for the simultaneous treatment of small-scale and large-scale interfaces. *International Journal for Numerical Methods in Fluids*, 75(8):547–574, 2014.
Nadiv C. and Semiat R. Batch settling of liquid-liquid dispersion. *Industrial & Engineering Chemistry Research*, 34(7):2427–2435, 1995.
Noïk C., Palermo T., and Dalmazzone C. Modeling of liquid/liquid phase separation: Application to petroleum emulsions. *Journal of Dispersion Science and Technology*, 34(8):1029–1042, 2013.
Palermo T. Le phénomène de coalescence. etude bibliographique. *Oil & Gas Science and Technology*, 46(3):325–360, 1991.
Polderman H. and Bouma J. Design rules for dehydration tanks and separator vessels. In *SPE Annual Technical Conference and Exhibition*. 1997.
Ramkrishna D. *Population balances: Theory and applications to particulate systems in engineering*. Elsevier, 2000.
Roe P. Characteristic-based schemes for the Euler equations. *Annual Review of Fluid Mechanics*, 18(1):337–365, 1986.
Sweby P. High resolution schemes using flux limiters for hyperbolic conservation laws. *SIAM Journal on Numerical Analysis*, pages 995–1011, 1984.
Toro E. *Riemann Solvers and Numerical Methods for Fluid Dynamics: A Practical Introduction*. Springer Verlag, 2009.
Van Leer B. Towards the ultimate conservative difference scheme. II. monotonicity and conservation combined in a second-order scheme. *Journal of Computational Physics*, 14(4):361–370, 1974.
Vié A. *Simulation aux grandes échelles d'écoulements diphasiques turbulents à phase liquide dispersée*. Ph.D. thesis, Institut National Polytechnique de Toulouse, Toulouse, 2010.
Vié A., Jay S., Cuenot B., and Massot M. Accounting for polydispersion in the eulerian large eddy simulation of the two-phase flow in an aeronautical-type burner. *Flow, Turbulence and*

Combustion, 90(3):545–581, 2013.

Weller H.G., Tabor G., Jasak H., and Fureby C. A tensorial approach to computational continuum mechanics using object-oriented techniques. *Computer in Physics*, 12(6):620–631, 1998.

Williams F A. Spray combustion and atomization. *Physics of Fluids (1958-1988)*, 1(6):541–545, 1958.

Yeoh G., Cheung C., and Tu J. *Multiphase flow analysis using population balance modeling: Bubbles, drops and particles*. Elsevier, 2014.